

# ATMOSPHERIC CORRECTION OF AIRBORNE PASSIVE MEASUREMENTS OF FLUORESCENCE.

F. Daumard<sup>a,\*</sup>, Y. Goulas<sup>a</sup>, A. Ounis<sup>a</sup>, R. Pedros<sup>b</sup>, I. Moya<sup>a</sup>

<sup>a</sup> LMD-CNRS, Ecole Polytechnique, 91128 Palaiseau – France, (fabrice.daumard, yves.goulas, ounis, ismael.moya)@lmd.polytechnique.fr

<sup>b</sup> Universitat de Valencia, Departament de Fisica de la Terra i Termodinamica, Valencia – Spain, Roberto.Pedros@uv.es

**KEY WORDS:** Fluorescence, Airborne Measurements, Altitude Effects, MODTRAN, AirFlex

## ABSTRACT:

A new instrument for passive remote sensing of sunlight-induced fluorescence took part in a series of airborne measurements during the summer 2005 (SEN2FLEX campaign). It measured for the first time the chlorophyll fluorescence emission over a succession of cultivated fields. The sensor is based on the Fraunhofer line discrimination principle, applied to the atmospheric oxygen absorption bands at 687nm and 760nm.

Nadir viewing measurements made at various altitudes (300m-3000m) showed a continuous increase of the band depths when increasing the altitude. Among several radiative transfer models of the atmosphere, MODTRAN 4 was chosen to account for these altitude effects, because of its resolution (2cm-1) and its capability to describe multiple scattering. In order to validate the model, a data base was build up using ground measurements of the depth of the oxygen absorption band at 687 and 760 nm during a diurnal cycle.

In this paper, we compare depths measured at the ground level with the MODTRAN 4 predictions. Local aerosol contents were retrieved from spectroradiometric measurements and included in the model. It is conclude that MODTRAN 4 is able to accurately describe the variation of the atmospheric oxygen absorption bands at 760 nm. The depth variation at 687 nm are also retrieved, but with a lower accuracy, due in part to the uncertainties of the spectral characteristics of the sensor. The sensitivity to several parameters, including aerosols, water content and ozone was studied.

## 1. INTRODUCTION

The vegetation holds an important place in the cycle of carbon, in such a way that the gaseous exchange between vegetation and atmosphere is one of the key parameters of climate modeling. A way to quantify and identify these exchanges is to study the photosynthesis activity: large-scale measurement of the vegetation's photosynthesis activity may provide important information to improve the knowledge of the vegetation's role in the carbon cycle.

Fluorescence is a deexcitation mechanism in competition with photochemical conversion. Therefore, measuring the fluorescence emitted by the vegetation is one way to assess its photosynthesis activity.

The passive fluorescence measurement, which uses the sun as the light source, is a promising technique to provide large-scale data. Under natural sunlight illumination, the amount of chlorophyll fluorescence emitted by the vegetation represents less than 1% of the radiance of the vegetation: it is a very weak signal. However, at certain wavelengths where the solar spectrum is attenuated, the fluorescence signal becomes not negligible and can be quantified by the measurement of the filling of the band. This is the FLD principle (Fraunhofer Line Discriminator) (Plascky, 1975) which was adapted to the atmospheric oxygen absorption bands (Moya et al., 1998) in order to quantify the chlorophyll fluorescence signal. The sunlight-induced fluorescence is obtained by comparing the depth of the atmospheric oxygen absorption band in the solar irradiance spectrum to the depth of the band in the radiance spectrum of the plants. In the last ten years, several passive

instruments were proposed and used (Moya et al., 1998, 2004; Louis et al., 2005) successfully to measure the fluorescence of the vegetation at short distances (<50m).

An airborne campaign lasting several days SEN2FLEX (SENtinel-2 and FLuorescence EXperiment) was carried out in summer 2005 to study the spatial variability of the fluorescence signal. The measurements were made on various crops during several days. The preliminary results showed the reproducibility of the measurements made at the same altitude and a very good correlation between depths and the calculated NDVI (Normalized Difference Vegetation Index). See accompanying paper (Moya et al., 2006). To study the air mass effect on the band depth, a flight along the same track was made at different altitudes: 327m, 640m, 1242m, and 3119m.

The aim of this paper is to present a correction model of altitude effects on the depth of A and B atmospheric oxygen absorption bands.

## 2. MATERIAL AND METHODS

The sunlight's path length varies during the day with the solar zenith angle and so does the amount of O<sub>2</sub> on the optical path crossed by the light to reach the ground. It results in a diurnal variation of depths (Moya et al., 2004).

In order to validate the model, a set of diurnal cycles of band depths have been acquired. The model is regarded as accounting for the atmospheric effects if it succeeds in predicting these diurnal cycles.

\* Corresponding author. fabrice.daumard@lmd.polytechnique.fr

## 2.1 Diurnal Cycle Measurements

**Sensor:** The sensor used to acquire the diurnal cycle, TerFlex, is identical to the one used for flights. It is a six channels sensor, each one constituted by a photodiode (Si PIN) and a narrow band interference filter. The set of filters used in the optical head is maintained at a constant temperature of 40°C to avoid any shifting or broadening of the transmission filters. Terflex provides a simultaneous flux measurement in the six channels ensuring time correlation. For both A and B bands, three optical measurements are performed: one in-band and two off-band, on the continuum. The use of two filters out of the band allows to interpolate the reflectance within the band. See Table 1 for filters details.

Position	FWHM	Name	Use
685.17 nm	Off band	0.5 nm	B687 Compute the B-band depth.
687.03 nm	In band	0.5 nm	
757.46 nm	Off band	1 nm	B760 Compute the A-band depth.
760.55 nm	In band	1 nm	
694.16 nm	Off band	5.8 nm	R695 Compute the in band reflectance.
770.55 nm	Off band	2.25 nm	

Table 1. Filter Position

Terflex has been calibrated before and after the campaign. For each channel, the flux intensity and spectral transmission have been measured using a spectrally calibrated source (LiCor 1800-02). The calibration uncertainty, about 0.7% in the B-band and 1.5% in the A-band, is the standard deviation of several independent measurements.

**Experimental Setup:** The measurement campaign took place on 1, 2, 3 June 2005, at Las Tiesas-Anchor site (Barraix, Spain) ( $39^{\circ} 03' 30''$  N;  $2^{\circ} 05' 24''$  W) under clear-sky conditions. TerFlex was installed on the ground in a vertical position: about 1.5 m height from the ground (see fig. 1).



Figure 1. TerFlex sensor in its measuring configuration.

At that height, the spot size on the target was about 20 cm. The instrument was north-to-south oriented to avoid any shading of the target. TerFlex was targeting a lambertian surface acquiring fluxes in the six channels from 10:00 to 17:00 local time. The lambertian reference (Spectralon, LabSphere) ensures that the reflexion coefficient is the same for each channel and avoids directional effects. In this manner, the band depths are simply defined by the following ratio:

$$\text{Depth} = \frac{\text{Flux}_{\text{Off band}}}{\text{Flux}_{\text{In band}}} \quad (1)$$

**Aerosols Measurements:** During the campaign, the aerosol properties have been monitored by the Solar Radiation Team of the University of Valencia. Using the technique described in (Martinez-Lozano et al., 2001) the aerosol optical thickness (AOT) has been retrieved from the measurements of the solar direct irradiance with a LiCor 1800 spectroradiometer. The ozone content was measured with a photometer (Microtops II) and the relative humidity was measured in a meteorological tower and with several radio soundings. By inverting the Mie theory included in the OPAC model (Optical Properties of Aerosols and Clouds) (Hess et al. 1998), the aerosol model and the particle densities that better fit the measured AOT were obtained. Several aerosol models were considered, including “continental”, “continental clean”, “maritime”, “maritime clean”, “mixture of continental and maritime”, “desert outbreak” (Saharan dust). Once identified the aerosol composition, the Mie theory was used to produce the aerosol properties (absorption spectrum, extinction spectrum, asymmetry factor, phase function) required for a more accurate description of the aerosols in MODTRAN.

## 2.2 Modeling :

Among several radiative transfer models of the atmosphere, MODTRAN 4 (v1r1) (MODerate Spectral Resolution Atmospheric TRANsmittance Algorithm) was chosen to correct for these altitude effects, because of its resolution,  $2 \text{ cm}^{-1}$ , and its capability to describe multiple scattering.

The MODTRAN input file is generated in order to reproduce the conditions of measurement. Table 2 shows the main parameters of the MODTRAN configuration file used.

Parameter :	Value :
Calculation Option	MODTRAN correlation-k
Type of Atmospheric Path	Slant Path to Space or Ground
Atmosphere	MidLat Summer
Mode of Execution	Radiance w/ Scattering
Scattering Algorithm	DISORT
DISORT streams	16
Temperature at First Boundary	298
Surface Albedo	1
FWHM of Slit Function	1 cm $^{-1}$

Table 2. Main parameters of the MODTRAN input file.

To describe the aerosol content, MODTRAN divide the atmosphere into four vertical regions. The first one is the boundary layer. The vertical distribution of the aerosol concentration in the boundary layer is drive by the “surface meteorological range” which characterizes the visibility; this parameter is called “VIS” in MODTRAN. This parameter provides a way to increase or decrease the amount of aerosol in the boundary layer. Larger values of “VIS” reduce aerosols effects, while smaller values increase aerosol effects. For hazy conditions (“VIS” from 2 to 10 km) the boundary layer aerosol concentration is assumed to be independent of height up to 1 km with a pronounced decrease above that height. For “VIS” from 23 to 50 km (clear to very clear conditions), the vertical distribution of concentration is taken to be exponential. Above the boundary layer, the aerosol characteristics become less sensitive to weather and geography variations. At these altitudes, changes are more a result of seasonal variations. The “VIS” parameter is set using the Koschmieder formula:

$$VIS = \frac{\ln(1/\varepsilon)}{Extc_{550} + 0.01159} \quad (2)$$

Where  $Extc_{550}$  is the retrieved aerosol extinction coefficient at 550 nm,  $\varepsilon=0.02$  is the threshold contrast in MODTRAN and  $0.01159 (\text{km}^{-1})$  is the surface Rayleigh scattering coefficient at 550 nm.

For each region, MODTRAN allows assigning aerosols properties such as extinction spectrum, absorption spectrum, asymmetry factor and phase function. This feature is used in order to have a better description of the aerosol loading.

For calculation, we used the “Correlation-k” (Slow) option of MODTRAN, which improves the accuracy of radiance calculation (Berk et al., 1999), mainly in the absorption zone. The algorithm used for the multiple scattering is DISORT (DIScrete Ordinate Radiative Transfer) (Stamnes et al, 1988), it allows a better precision than the default algorithm (Modtran 2). All the parameters driving the accuracy of the calculation are set to ensure the best precision.

The output of the computation is the radiance spectrum at the sensor level. In order to obtain fluxes, this spectrum is integrated over the measured transmission function of each TerFlex channel. Then the depths predicted by MODTRAN can be obtained.

### 3. RESULTS AND DISCUSSION

As the results are fairly the same for the entire campaign, we mainly focus on the results of the 1<sup>st</sup> of June

#### 3.1 Altitude effects

**Fluxes:** The air column between the vegetation and the sensor modify the signal coming from the vegetation: it absorbs part of the signal ( $O_2$  absorption) and contributes to it through its albedo. In order to assess these effects, flights were made along the same track at different altitudes: 327m, 640m, 1242m, and 3119m. Figures 2 show the evolution of the in-band and off-band fluxes measured on the vegetation versus the altitude. In the A-band (Fig. 2.b) the fluxes decrease with altitude, this is the effect of the oxygen absorption.

Figure 2.a shows that in the B-band the fluxes increase with altitude. For the B-band, the signal coming from the vegetation is very weak because of the low reflectance of the vegetation in this wavelength range. Thus, the behaviour of fluxes is dominated by the contribution of the radiance of the atmosphere between the target and the sensor and not by the effect of absorption.

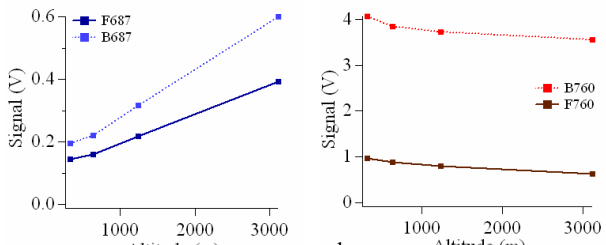


Figure 2. Radiances measured over the same field vs. altitude (3rd of June).  
a. B-band.  
b. A-band.

**Depths:** Figures 3 shows that the depths increases with the altitude, this behaviour is due to the absorption of the oxygen.

This is not a negligible effect: in the A-band, measuring the depths at an altitude of 3 km instead of the ground level leads to a variation on depth bigger than the variations induced by vegetation. In the B-band, the variations induced by vegetation are of the same order of magnitude. The variation of depths due to fluorescence at ground level is about 7.6% and 2.5% in the B-band and A-Band respectively.

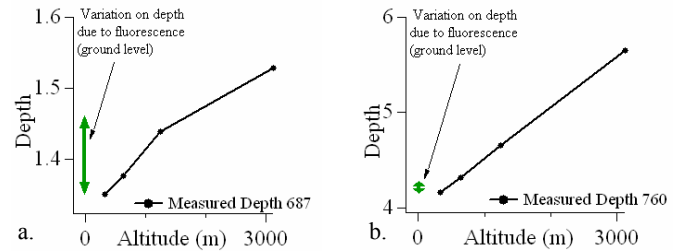


Figure 3. Depths measured over the same field vs. altitude (3<sup>rd</sup> of June).  
a. B-band.  
b. A-band.

The altitude effect is so strong compared to the fluorescence signal that a model is needed to take into account this effect.

#### 3.2 Measured Diurnal Cycle

Figure 4 shows diurnal cycle records in both bands for the 1<sup>st</sup> of June from 11:00 to 17:00, local time. The depth of the A-band ranges from 4.1 (noon) to 5.26 (11:00 a.m.). Thus, the diurnal cycles imply a variation of 28% from the minimum to the maximum. In turn, the B-band values ranges from 1.32 (noon) to 1.40 (11:00 a.m.), which means a variation of 6%.

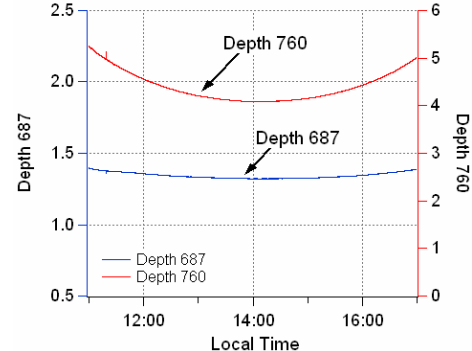


Figure 4. Diurnal cycle recorded on the 1st of June.

The uncertainty on these values, due to the calibration of the sensor, is about 0.7% in the B-band and 1.5% in the A-band.

#### 3.3 Measurement of the Channel Transmission Function

**Spectral Calibration:** Great attention has been paid to the measurement of the transmission functions because of their narrow bandwidth. A small shift of the transmission functions could dramatically change the computed flux, especially for the in-band filters. The transmission functions were measured with a HR4000 spectrometer (Ocean Optics). The spectral instrumental function of the HR4000 has been measured, using the atomic lines at 763.51 nm (Ar) and 690.67 nm (Hg) of an Hg(Ar) calibration lamp (Oriel Instruments, France). The shape of the instrumental function was found different for each atomic line with the same FWHM, of about 0.5 nm. The actual transmission functions of each channel were retrieved after

deconvolution of the measured transmission spectra by the instrumental response function of the spectrometer. The deconvolution process has reduced the FWHM of the filters of about 37% and has corrected their shape.

A final accuracy of 0.1nm is estimated for the actual channel transmission.

**Radiometric Calibration:** Terflex has been calibrated against a black body (Li-Cor 1800-02, NE, USA), so that the flux obtained for each channel is comparable to the others.

### 3.4 Sensitivity Studies

The effect of the air mass depends on several parameters including the sensor's altitude, the sun elevation and the state of the atmosphere. The sensitive parameters of the model are the ones that could modify the scattering and absorption properties of the atmosphere. It is necessary to evaluate their influence on the computed band depths and to determine whether they need to be measured or not. The results will be compared both to the change of the depths due to fluorescence and to the accuracy of the measurement.

**Atmosphere Model Sensitivity:** MODTRAN 4 has six reference atmospheres. Table 3 present depths at solar noon the 1<sup>st</sup> of June computed with each reference atmosphere. It shows that the standard deviation for the B-band and the uncertainty on measurements are of the same order of magnitude. Attention should be paid to the choice of atmosphere model. As the campaign took place in Spain on summer, the MidLat Summer model is chosen (45N latitude, July).

Model Atmosphere	Depth B-band	Depth A-band
US Standard 1976	1.346	4.089
Tropical	1.357	4.076
MidLat Summer	1.354	4.059
MidLat Winter	1.342	4.126
SubArtic Summer	1.348	4.043
SubArtic Winter	1.333	4.104
Standard Deviation	0.64%	0.74%
Maximum Variation	1.6%	2%

Table 3. Band depths computed with MODTRAN at solar noon the 1<sup>st</sup> of June for each atmospheric model.

**Water Content :** In Table 4 the band depth at noon are calculated for various values of the water vapour column, from 0.001 g.cm<sup>-2</sup> to 6 g.cm<sup>-2</sup> (Noël et al., 2005). The measured water content value is 1.4g.cm<sup>-2</sup> giving values of the band depths of 1.354 and 4.058 for the B-band and A-band respectively. Table 4 show that the variations for the A-band are negligible. For the B-band the standard deviation of depth is not negligible compared to the uncertainty on the measurements.

However, the depths computed with the default value of water content are close to the ones obtained with the actual value. One can conclude that the default value could be used without significant errors if the water content measurement is not available.

Water content (g.cm <sup>-2</sup> )	Depth B-band	Depth A-band
Default	1.3544	4.05858
0.001	1.3516	4.05844
1	1.3533	4.05854
6	1.3568	4.05851
Measured : 1.4	1.3539	4.05853
Standard Deviation	0.2%	<0.02%

Table 4. Band depths versus the water content computed at solar noon the 1<sup>st</sup> of June.

**Ozone content:** In Table 5 the band depths are calculated for various values of the ozone content from 0.2 atm-cm to 0.5 atm-cm. The standard deviations of the band depths are small for large variation of the ozone content. Furthermore, the measured ozone content is 0.284 atm-cm at noon giving 1.3545 and 4.0584 for the B-band and A-band depths respectively. These values are close to those obtained with default setting. One can conclude that the measurement of the ozone content is optional and that the default setting can be used.

Ozone content (atm-cm)	Depth B-band	Depth A-band
Default	1.3544	4.0586
0.2	1.3547	4.0586
0.35	1.3544	4.0582
0.5	1.3541	4.0577
Measured: 0.284	1.3545	4.0584
Standard Deviation	<0.3%	<0.2%

Tables 5. Band depths in function of the ozone content computed at solar noon the 1<sup>st</sup> of June.

**Aerosols:** The aerosol data acquired during the campaign represent the integrated aerosol properties along the whole atmospheric column but does not give information on their vertical distribution. Consequently, they are included in MODTRAN as one single layer, discarding the others. By default, in MODTRAN, the first layer extends from 0 km to 3 km. In order to estimate the effect of aerosols vertical distribution, the variations of the band depths with the altitude of the aerosol layer have been investigated. Setting the aerosol layer at an altitude of 5 km instead of 3 km will change the average optical path length. The depth of the bands should vary consequently. It is the same issue for the layer thickness. Figure 5 presents the variation of depths when changing the altitude of the aerosol layer from 0 km to 5 km. Setting the altitude of the main aerosol layer to 5 km is not realistic physically. Calculation is made to have an increase of the effect of the aerosols distribution. The vertical scales of the graphs are defined so that the variations induced by fluorescence represent the full scale.

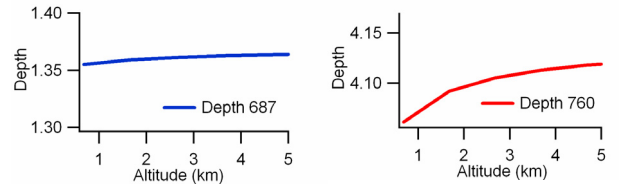


Figure 5. Band depths versus the aerosol layer altitude.

Figure 5 shows that the variation of depth induced by setting the altitude of the layer to 5 km instead of 0 km is about 0.7% for the B-band and 1.5% for the A-band. The variations are important, especially in the A-band where the maximum variation represents about the half of the effect due to

fluorescence. For the B-band the maximum variation represents less than 10% of the variation due to fluorescence. Figures 6 show that the effects are similar on the whole when one increases the aerosol layer thickness.

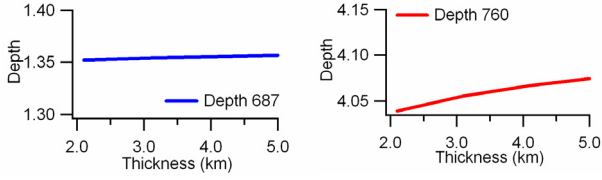


Figure 6. Band depths versus the aerosol layer thickness.

There is no measurement allowing the choice of a configuration rather than another. The LIDAR didn't function during this part of the campaign. Thus, the default configuration will be used: a layer extending from 0 to 3km.

The aerosols properties used were detailed retrieved from the measurements of AOT with the OPAC model as described before. The retrieving of such detailed properties might be unnecessary. To assess the improvement induce by the use of detailed properties, the depths obtained with this description of aerosols were compared to the depths obtained with the standard aerosol models. MODTRAN has three standard aerosol models: "Rural", "Maritime" and "Urban" (Berk et al, 1999). They provide aerosol extinction characteristic of an air mass that has just moved through one of these types of areas. The parameter "VIS" is used to drive the models. Larger values of "VIS" reduce the aerosols effects, while smaller values increase the aerosol effects.

In transmission mode, MODTRAN separately tabulates the transmission due to aerosols. The AOT can be deduced from this calculation by the negative of the logarithm (Conant et al.). Tables of visibility versus AOT at 700 nm were computed for each aerosol model. Then diurnal cycles were computed using the visibility matching the measured AOT. Table 6 shows, for the 1<sup>st</sup> of June, the maximum deviation of depth over a diurnal cycle computed with each standard aerosol model instead of the aerosol properties retrieved. The mean AOT was 0.1508.

Model	Rural	Maritime	Urban
VIS matching mean measured AOT (700 nm)	33.655 km	40.129 km	35.519 km
Max deviation for a diurnal cycle B-Band	0.8 %	0.8 %	0.3 %
Max deviation for a diurnal cycle A-Band	2.2 %	2.3 %	1 %

Table 6. Comparison between standard aerosol model and accurate properties of aerosols.

Although the rural model seemed to be more adapted to describe the conditions of the measurement, Table 6 shows that the model that best fits the data is the urban model. This shows that the retrieving of detailed aerosols properties is necessary because we wouldn't be able to choose a priori the built-in model that would best represent the aerosols conditions during the measurements.

### 3.5 Diurnal Cycle Modeling

In order to validate the model, several simulations of the diurnal cycle were computed from 9:00 to 15:00, solar time, using 30 min steps.

Figures 7 and 8 compare modeled diurnal cycles and measured ones. The two dotted curves represent the uncertainty of the measurement. The error bar represent the uncertainty due to the resolution of the spectrometer used to acquire the transmission functions estimated at 0.1 nm.

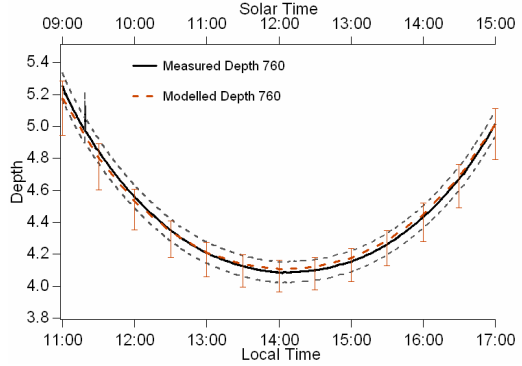


Figure 7. Comparison between measured and modeled diurnal cycle in the A-band.

Figure 7 shows that the shape of modeled curve for the A-band is in agreement with the experimental one. The model uncertainty is comparable to the measurements uncertainty.

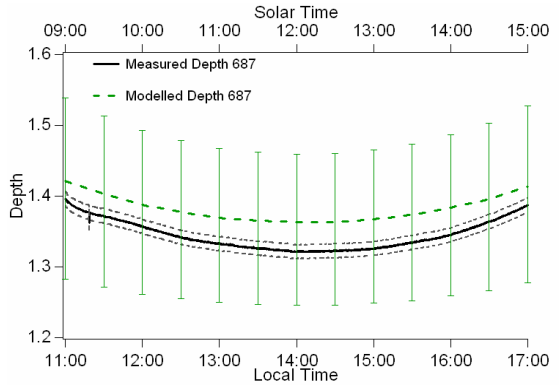


Figure 8. Comparison between measured and modeled diurnal cycle in the B-band.

Although the error bars are large, the figure 8 shows that the shape of the modeled curve is different from the measured one. That may signify that there are some unknown factors that may influence the depth of the B-band. An assumption is that MODTRAN may underestimate the radiance of the atmosphere. The undervaluation of this radiance leads to the over-estimate of the depth, as seen on Fig 8. This problem does not exist in A-band where the absorption is much stronger.

Nevertheless, taking into account the error bar, the model is in agreement with the experimental values. The B-band is narrow implying that the model is highly dependent on the accuracy of the actual spectral shape of the filters. In order to have error bar of the same order of magnitude for both the model and the measurements, it would be necessary to characterize the filters with an accuracy of about 0.01 nm.

In both cases, the depths obtained with MODTRAN are in agreement with the measured data within the uncertainty range. The model is able to reproduce the diurnal cycle for both bands, yet with less accuracy for the B-band. One can conclude that the model takes into account the atmospheric effects that influence the measurements so the corrections can be computed using MODTRAN 4.

### 3.6 Application to Altitude Effects

There are two types of correction: an altitude correction to correct the effect of atmospheric oxygen absorption and a time correction. This time correction allows to take into account the fact that for each altitude, as the measurements were not been made at the same time, the sun position was not the same.

**Altitude correction:** This correction allows to retrieve the fluxes at the ground level and is calculated with (3).

$$C_{alt} = \frac{Depth_{ground}}{Depth_{alt}} \quad (3)$$

Where  $Depth_{ground}$  is the depth computed at the ground level,  $Depth_{alt}$  is the depth computed at the measurement altitude of measure and  $C_{alt}$  is the correction coefficient (multiplicative) for the altitude effects.

**Time correction:** A correction computed with (4) is required because the measurements were not made at the same time.

$$C_{time} = \frac{Depth_{reference-time}}{Depth_{measure-time}} \quad (4)$$

Where  $Depth_{reference-time}$  is the depth computed at a reference time,  $Depth_{measure-time}$  is the depth computed at the measure time and  $C_{time}$  is the correction coefficient (multiplicative).

All the depths in (3) and (4) are MODTRAN-computed.

Both corrections have been computed and applied to the measurements. Figures 9 shows measured and corrected depths acquired on the same bare field versus the altitude.

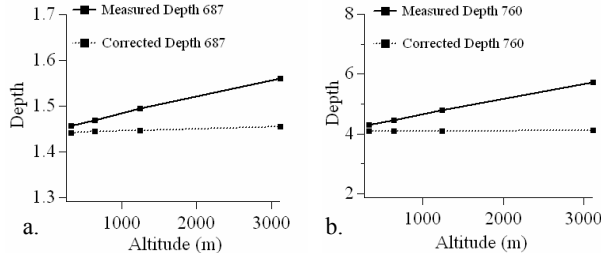


Figure 9. Depths acquired on bare field vs. altitude

a. B-band (3rd of June).  
b. A-band (3rd of June).

Figures 9 show that the model is able to correct for the band depths: the corrected depths retrieved coincide for the four altitudes of measurements.

### 4. CONCLUSION

MODTRAN 4 can be used to account for the altitude effects on the A and B oxygen absorption bands depths. This study shows that the model does not depend critically on parameters such as water content and ozone content. Good results were obtained on both bands depths for the altitude correction up to 3km. This altitude represents about 50% of the atmospheric effects. The diurnal cycles measured with TerFlex generate a valuable set of data to validate the model for atmospheric corrections in long-range passive fluorescence measurements. The measurement of

the channels transmission function is a critical issue for the model accuracy. This point will be further improved in a forthcoming work.

### REFERENCES

- Berk, A., Anderson G.P., Acharya, P.K., Chetwynd, J.H., Bernstein, L.S., Shettle, E.P., Matthew, M.W., and Adler-Golden, S.M., 1999. MODTRAN4 user's manual.
- Conant, J., Iannarilli, F., Bacon, F., Robertson, D., and Bowers, D. PPACS – A System To Provide Measured Aerosol/Molecular Conditions To EO/IR Simulations. Aerodyne Research INC.
- Hess, M., Koepke, P., and Schult, I., 1998. Optical Properties of Aerosols and Clouds: The Software Package OPAC. *Bulletin of the American Meteorological Society*, Vol. 79, N° 5, pp. 831-844
- Louis, J., Ounis, A., Ducruet, J.M., Evain, S., Laurila, T., Thum, T., Aurela, M., Wingsle, G., Alonso, L., Pedros, R., and Moya, I., 2005. Remote sensing of sunlight-induced chlorophyll fluorescence and reflectance of Scots pine in the boreal forest during spring recovery. *Remote Sensing of Environment*, Vol. 96, pp. 37 – 48
- Martinez-Lozano, J.A., Utrillas, M. P., Tena, F., Pedros, R., Canada, J., Bosca, J.V., and Lorente, J., 2001. Aerosol optical characteristics from a summer campaign in an urbano-coastal Mediterranean area. *Geosciences and Remote Sensing*, Vol. 32 No. 7, pp. 1573-1585
- Moya, I., Camenen, L., Latouche, G., Mauxion, C., Evain, S., and Cerovic, Z.G., 1998. An instrument for the measurement of sunlight excited plant fluorescence. *Photosynthesis: Mechanisms and Effects*. Dordrecht, Kluwer Acad. Pub., pp. 4265-4270
- Moya, I., Camenen, L., Latouche, G., Goulas, Y., Gerovic, Z.G., Latouche, G., Flexas, J., and Ounis, A., 2004. A new instrument for passive remote sensing 1. Measurements of sunlight-induced chlorophyll fluorescence. *Remote Sensing of Environment*, Vol. 91, pp. 186-197
- Moya, I., Daumard, F., Moise, N., Ounis, A., and Goulas, Y., 2006. First airborne multiwavelength passive chlorophyll fluorescence measurements over La Mancha (Spain) fields.
- Noël, S., Buchwitz, M., Bovensmann, H., and Burrows, J. P., 2005. Validation of SCIAMACHY AMC-DOAS water vapour columns. *Atmospheric Chemistry and Physics*, Vol. 5
- Plascyk, J.A., 1975. The MKII Fraunhofer line discriminator (FLD-II) for airborne and orbital remote sensing of solar-stimulated luminescence. *Opt. Eng.*, Vol.14, pp. 113-120
- Stamnes, K., Tsay, S-C., Wiscombe, W., and Jayaweera, K., 1988. Numerically stable algorithm for discrete-ordinate-method radiative transfer in multiple scattering and emitting layered media. *Applied Optics*, Vol. 27, N° 12., pp 2502-250